ELSEVIER

Biochimica et Biophysica Acta 1418 (1999) 133–146

BIOCHIMICA ET BIOPHYSICA ACTA
BBA

Probing DMPG vesicle surface with a cationic aqueous soluble spin label

Karin A. Riske [a], Otaciro R. Nascimento [b], Miroslav Peric [c], Barney L. Bales [c], M. Teresa Lamy-Freund [a,*]

[a] *Instituto de Física, Universidade de São Paulo, CP 66318, CEP 05315-970, São Paulo, SP, Brazil*
[b] *Instituto de Física de São Carlos, Universidade de São Paulo, CP 780, CEP 13560-970, São Carlos, SP, Brazil*
[c] *Department of Physics and Astronomy, California State University at Northridge, Northridge, CA 91330, USA*

Received 21 January 1999; accepted 22 January 1999

Abstract

A small, highly aqueous soluble, deuterated, cationic spin label, 4-trimethylammonium-2,2,6,6-tetramethylpiperidine-d_{17}-1-oxyl iodide (dCAT1), was used to directly monitor the negatively charged DMPG vesicle surface in order to test a recent suggestion (Riske et al., Chem. Phys. Lipids, 89 (1997) 31–44) that alterations in the surface potential accompanied apparent phase transitions observed by light scattering. The temperature dependence of the label partition between the lipid surface and the aqueous medium indicated an increase in the surface potential at the gel to liquid–crystal transition, supporting the previous suggestion. Results at the phase transition occurring at a higher temperature were less definitive. Although some change in the dCAT1 ESR spectra was observed, the interpretation of the phenomena is still rather unclear. DMPG surface potentials were estimated from the dCAT1 partition ratios (surface label moles/total label moles), using a simple two-sites model, where the electrostatic potential is zero everywhere but at the vesicle surface, and the interaction between the spin label and the membrane surface is chiefly electrostatic. The Gouy–Chapman–Stern model predicts surface potentials similar to those observed, although the measured decrease in the surface potential with ionic strength is somewhat steeper than that predicted by the model.

Keywords: DMPG; Spin label; Phase transition; Surface potential

1. Introduction

Under physiological conditions, most cell membranes have a negative net charge due to the dominance of acidic lipid headgroups. Hence, anionic phospholipids have been widely used as model systems for biological membranes, considering that the charged character of the lipids might be rather important in many of the membrane roles (see, for instance, [1]). Phosphatidylglycerol is the most abundant anionic phospholipid present in prokaryotic cell membranes, having been extensively studied as a charged model membrane [2–5], presenting, under physiological conditions, some properties similar to those of the ubiquitous phosphatidylcholine with the same acyl chains [2,6,7].

On the other hand, the thermotropic behavior of DMPG dispersions at different conditions of pH, ionic strength, lipid concentration and time of incubation at a certain temperature [2,4,7–13], has re-

* Corresponding author. Fax: +55-11-813-4334;
E-mail: mtfreund@fge.if.usp.br

0005-2736/99/$ – see front matter
PII: S0005-2736(99)00019-X

vealed itself to be a very rich and interesting field of physicochemical research. Although biological membranes are composed of many different lipids, the lipid phase separations that are likely to occur physiologically, could create domains where the structural properties of a given lipid might be fundamental to a certain biological function.

In a range of ionic strength, freshly prepared dispersions of DMPG were found to present a rather complex behavior [4,10,12], that was interpreted by some authors [10,12] as two different phase transitions between 5°C and 45°C: the well known gel to liquid–crystal transition at T_m, and another one, called the post-transition, at T_{post}. Both transitions could be observed by 90° light scattering [12] and differential scanning calorimetry (DSC) [10]. In a previous work [12], it was suggested that, at least at T_m, the decrease in light scattering could be due to an increase in the vesicle surface electrostatic potential upon the thermal phase transition. Hence, among the different forces that act between two charged DMPG vesicles, the increase in the electrostatic double layer repulsion would be the triggering factor responsible for the low scattering window observed between T_m and T_{post}. Accordingly, a simple Gouy–Chapman–Stern model was put forward for the main transition, considering that the melting of the hydrocarbon chains could change both the area per lipid headgroup and the Na^+–PG^- association constant, therefore modifying the electrical surface potential of the DMPG vesicle. The phenomena occurring at T_{post} was more difficult to be rationalized, as there was no indication of any microscopic structural change at that temperature [12].

In an effort to better understand the role of surface electrostatics in the phase transition of DMPG vesicles, in the present paper a small, highly aqueous soluble, deuterated, cationic spin label, dCAT1, was used to directly monitor the negatively charged DMPG vesicle surface. This strategy is based on those used for calculating surface potential with amphiphilic fluorescent or spin probes [14–19], but probing the physicochemistry of biological membranes from the 'outside'. Such a strategy provides an alternative view and most likely perturbs the membrane less than a probe incorporation into the membrane. Further, as a practical matter, many lipid soluble probes yield ESR spectra too immobilized to yield precise data.

Deuteration of the label reduces the unresolved hyperfine structure [20], making the spectral analysis and fitting more accurate. The temperature dependence of the partitioning of the label between the lipid surface and the aqueous medium was analyzed for various ionic strengths. The membrane partition ratio (surface label moles/total label moles) and the ESR spectra parameters for the dCAT1 in DMPG dispersions were compared with those obtained with the same spin label in sodium dodecyl sulfate (SDS) micelles.

Based on a simple two-sites model, assuming that electrostatics dominate the interactions between the spin label and DMPG, partition ratios were used to calculate the lipid vesicle electrostatic surface potential. The values so calculated are compared with those yielded by the Gouy–Chapman–Stern model.

2. Materials and methods

2.1. Materials

The sodium salt of the phospholipid DMPG (1,2-dimyristoyl-*sn*-glycero-3-[phospho-*rac*-glycerol, lot no. 140PG-115) and the spin label 16-PCSL (1-palmitoyl-2-(16-doxyl stearoyl)-*sn*-glycero-3-phosphocholine) were obtained from Avanti Polar Lipids (Birmingham, AL, USA). The deuterated spin label dCAT1 (4-trimethylammonium-2,2,6,6-tetramethylpiperidine-d_{17}-1-oxyl iodide) was purchased from CDN Isotopes (Quebec, Canada). SDS (sodium dodecyl sulfate) was from Sigma Chemical Co. (St. Louis, MO, USA). If not stated otherwise, the buffer system used was 10 mM Hepes (4-(2-hydroxyethyl)-1-piperizineethanesulfonic acid) adjusted with NaOH to pH 7.4. The ionic strength was calculated and measured to be 4 mM. Mille-Q Plus water (Millipore), pH 5.6, was used throughout.

2.2. Lipid dispersion preparation

A lipid film was formed from a chloroform solution of lipids, dried under a stream of N_2 and left under reduced pressure for a minimum of 2 h, to

remove all traces of the organic solvent. Vesicles were prepared by the addition of the desired buffer or water solution, with or without added salt, followed by vortexing above the phase transition temperature. When wanted, 0.1 mM of dCAT1 was added to the aqueous solution where the lipid dispersion was suspended, resulting in the exposure of all lipids to the spin label. (In the conditions used here, 10 mM DMPG in 10 mM Hepes buffer (pH 7.4), plus NaCl varying from 2 to 100 mM, preliminary results with small angle X-ray scattering indicated the absence of multilamellar liposomes).

2.3. 90° light scattering

A fluorimeter Hitachi F-3010 at a wavelength of 280 nm was used. The temperature was maintained with an external water bath Forma Scientific 2006, and measured with a Fluke 51 K/J thermometer placed inside the cuvette. For both light scattering and ESR, the experimental results shown here were obtained by varying the temperature from the higher to the lower value, and leaving the sample for at least 5 min at each temperature. Nevertheless, both experiments were found to be reversible, and identical results were obtained by increasing the temperature.

2.4. ESR spectroscopy

ESR measurements were performed with a Bruker EMX spectrometer. A field-modulation amplitude of 0.7 G and microwave power of 5 mW were used. This modulation amplitude broadened only the Gaussian component of the ESR line as expected [21]. The temperature was controlled to about 0.2°C with a Bruker BVT-2000 variable temperature device. The temperature was always monitored with a Fluke 51 K/J thermometer with the probe placed just above the cavity. The magnetic field was measured with a Bruker ER 035 NMR Gaussmeter, and the spectra were converted to a g-value scale with WINEPR software (Bruker). Most of the spectra shown here are aligned by the g-value. The spectral parameters were found by fitting each line to a Gaussian–Lorentzian sum function [22] taking advantage of the fact that the sum function is an accurate representation of a Gaussian–Lorentzian convolution, the Voigt function [20]. The hyperfine splitting, a_o, was taken to be one-half the difference in the resonance fields of the high- and low-field lines. The intrinsic (Lorentzian) linewidths and the line heights were determined from the fits [20]. Spectral subtractions were done using WINEPR software (Bruker). The data shown in Figs. 3 and 6 are results from at least three experiments with samples prepared at different times. In each experiment, two spectra were taken at each temperature and for each of these, two different subtractions of the type illustrated in Figs. 2 and 4 were carried out. The values are unweighted means of all of the results and the uncertainties are the standard deviations. When not shown (all data in Fig. 7 and some points in the other figures) the uncertainties are about the size of the symbols.

2.5. Surface potential calculation

Based on [14], a very simple two-sites model will be used here, where the spin label can be either in the aqueous phase, or close to the bilayer surface, with chemical potentials, in the ideal gas approximation, given by

$$\mu_{sol} = \mu^{o}_{sol} + kN_A T \ln(X_{sol})$$

$$\mu_{surf} = \mu^{o}_{surf} + kN_A T \ln(X_{surf}) + ZeN_A \Psi_{surf}$$

where μ^o means the standard chemical potential, k is the Boltzmann constant, N_A is the Avogadro's constant, T is the absolute temperature, Ze is the spin label charge ($Z=1$), and X_{sol} and X_{surf} mean the mole fractions of the spin label in the aqueous medium and at the membrane surface, respectively. In our two-sites model, the electrostatic potential is zero everywhere but at the vesicle surface, where the mean-field surface potential is $\Psi_{surf} = \Psi_o$. It will be assumed that there is no specific molecular interaction between the spin label and the membrane, that is, $\mu^o_{sol} \approx \mu^o_{surf}$, at least compared to the strong electrostatic term $eN_A\Psi_o$, as no surface dCAT1 could be detected for neutral DMPG at pH 1, or DMPG pH 7.4 at high ionic strength.

At equilibrium, $\mu_{sol} = \mu_{surf}$, so

$$\Psi_o = -\frac{kT}{e}\ln\left(\frac{X_{surf}}{X_{sol}}\right)$$

Considering that $X_{surf}/X_{sol} \approx$ (surface label moles/volume surface)/(free label moles/volume solution) = $(P/(1-P))(V_{sol}/V_{surf})$, where P is the calculated dCAT1 membrane partition ratio, namely (surface label moles)/(total label moles).

$$\Psi_o = -\frac{kT}{e}\ln\left(\frac{P}{(1-P)}\frac{V_{sol}}{V_{surf}}\right) \quad (1)$$

It will be assumed that $V_{sol} \approx V_{total}$, $V_{surf} = (ANh)$, where A is the area per lipid headgroup, N is the total number of lipids in V_{total}, and h is the thickness of the thin shell surrounding the lipids where dCAT1 can reside.

2.6. Gouy–Chapman–Stern model

The Gouy–Chapman–Stern electrostatic double layer theory (see, for instance, [23]) considers the electrostatic surface potential of a uniformly distributed infinite charged plane, with a surface charge density $\sigma = e\alpha/A$, where e is the elementary charge, α is the degree of DMPG dissociation and A is the area per lipid headgroup. Here, the degree of DMPG dissociation will depend on the PG^-–H^+ and PG^-–Na^+ binding constants:

$$K_H = \frac{[PGH]}{[PG^-][H^+]_o} \quad K_{Na} = \frac{[PGNa]}{[PG^-][Na^+]_o}$$

where [ ] refers to molar concentrations, and [ ]$_o$ to molar concentrations at the membrane surface. The latter can be estimated through the Boltzmann distribution:

$$[H^+]_o = [H^+]_\infty e^{-\frac{e\Psi_o}{kT}}$$

where $[H^+]_\infty$ is the proton concentrations at the bulk, k is the Boltzmann constant, T is the absolute temperature, and Ψ_o is the electrostatic surface potential. $[Na^+]_o$ can be calculated by a similar expression. So,

$$\alpha = \frac{[PG^-]}{[PG^-] + [PGH] + [PGNa]}$$

$$= \frac{1}{1 + (K_H[H^+]_\infty + K_{Na}[Na^+]_\infty)e^{-e\Psi_o/kT}} \quad (2)$$

The surface potential, in the Gouy–Chapman high potential approximation [23] in MKS units, is written as:

$$\Psi_o^{GCS} = -\frac{kT}{e}\ln\left(\frac{e^2}{2\times10^3\varepsilon\varepsilon_o kTN_A A^2 n}\right) \quad (3)$$

where ε is the medium dielectric constant, ε_o is the permittivity of free space, and n is the bulk ionic strength (in mol/l). Using Eqs. 2 and 3, we obtain an expression for α, that can be solved numerically:

$$\beta\alpha^3 + \alpha - 1 = 0$$

with

$$\beta = \frac{e^2}{2\times10^3\varepsilon\varepsilon_o kTN_A A^2}\left(K_{Na}\frac{[Na^+]_\infty}{n} + K_H\frac{[H^+]_\infty}{n}\right) \quad (4)$$

3. Results

Typical thermal profiles of the 90° light scattered by DMPG dispersions at different ionic strengths are presented in Fig. 1. Depending on the ion concen-

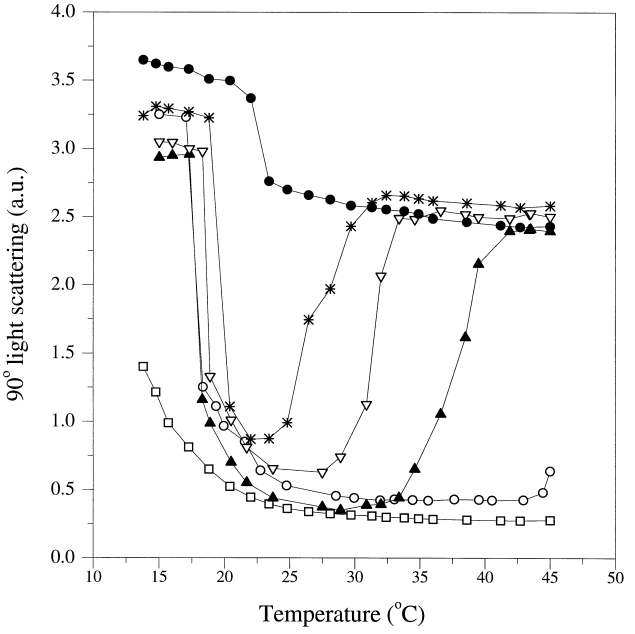

Fig. 1. Temperature dependence of 90° light scattering of 10 mM DMPG in different ionic strengths: (□) pure water; (○) buffer (10 mM Hepes, pH 7.4); buffer plus (▲) 2 mM, (∇) 5 mM, (*) 10 mM and (●) 100 mM NaCl. All samples contain 0.1 mM dCAT1.

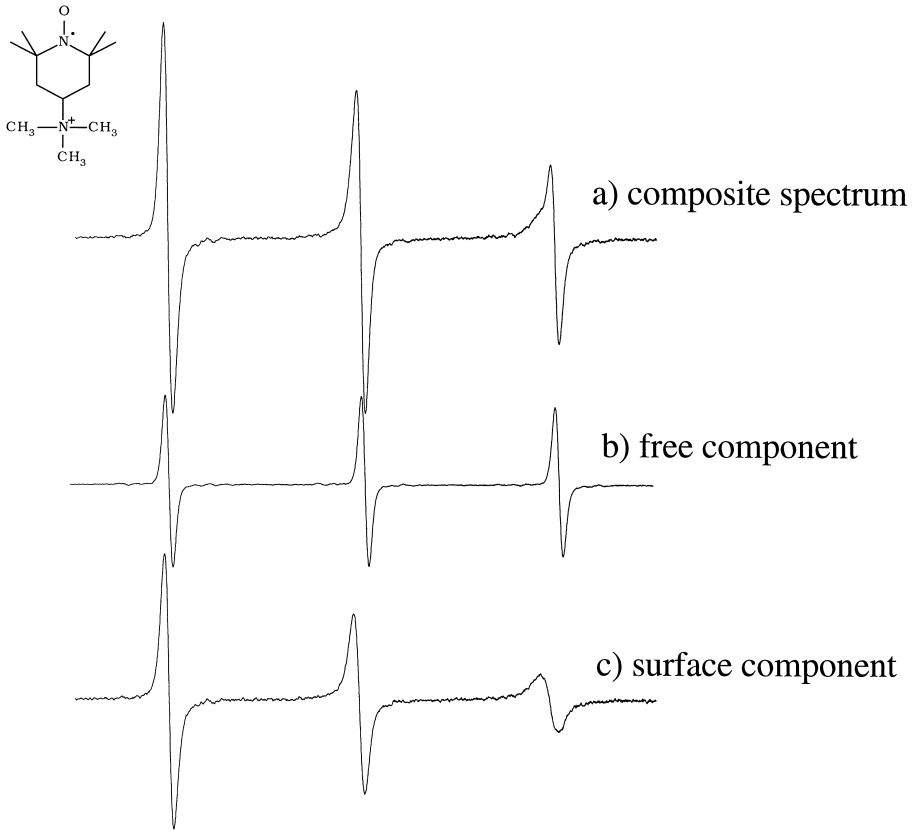

Fig. 2. (a) ESR spectra of 0.1 mM dCAT1 in 10 mM DMPG in buffer; (b) 0.1 mM dCAT1 free in buffer; (c) a typical ESR spectra subtraction, (a) minus (b). The free (b) and surface (c) components spectra are shown with the real relative intensities that they appear in the composite signal (a). Total spectra width 50 G, $T = 30°C$.

tration, two temperature transitions can be clearly observed: the main lipid transition around 20°C, and the post-transition at higher temperatures. Although the profiles shown here are similar to those presented in a previous paper [12], it is interesting to point out that whereas the DMPG main transition temperatures were identical to those found before, T_{post} was found to be dependent on the lipid batch used. With the one used in the present paper it was necessary to add 2 mM NaCl to the dispersions in 10 mM Hepes buffer (pH 7.4) to obtain a well defined post-transition (Fig. 1), very similar to that previously obtained with the lipid in pure Hepes buffer [12]. The strong dependence on the DMPG batch could possibly be related to a crucial dependence of T_{post} on the concentration of ions present in solution, which would be in accord with the large variation in T_{post} with the sample ionic strength. (The data shown in Fig. 1 were obtained in the presence of 0.1 mM dCAT1, but very similar results were obtained without the spin label, indicating that no significant variation was detected by the presence of the small additional concentration of ions due to the charged label).

The ESR spectrum obtained with dCAT1 in DMPG dispersions (Fig. 2a) was different from that yielded by the label in buffer solution (Fig. 2b), the former clearly indicating the presence of dCAT1 in more than one microenvironment. For most temperatures and ionic strengths, it was possible to decompose the dCAT1 spectrum obtained in DMPG dispersions into two components, one of them corresponding to the label free in solution, here referred as 'free' component. Fig. 2c shows a typical spectrum obtained after subtracting a weighted free signal (Fig. 2b) from the composite one (Fig. 2a). The weight of the free signal was varied until the resulting spectrum looked like a one

component signal and could be well fitted by a Voigt line shape [20]. This subtraction proceeds by trial and error, judging by eye the quality of the resultant spectrum; however, the fidelity of the spectrum is judged by the fact that the doubly integrated intensities and Gaussian linewidths of each of the three lines are required to be the same [20]. The fact that two well-separated spectra are obtained shows that the exchange rate between the two respective sites is slow on the ESR time scale. In the simple two sites model assumed here, the resulting spectrum (Fig. 2c) is yielded by the population of spin label close to the DMPG surface (an average value), henceforth called 'surface dCAT1'.

Decomposition of spectra into free and surface components was carried out for DMPG samples with different ionic strengths, at temperatures between 5°C and 45°C. Whenever possible, dCAT1 membrane surface partition ratios (P = surface label moles/total label moles) were calculated from the double integral of the ESR signals (Fig. 3). The values are compared to those obtained with dCAT1 in the 12.1 mM SDS in water system[1] (Fig. 4 shows the dCAT1 composite and subtracted spectra in SDS, at 25°C). The partition ratios calculated for temperatures below 17°C for DMPG–water, and 20°C for DMPG–buffer at the various salt concentrations are not very accurate, due to the similarity between the surface and free components of the ESR spectra (or to the rather small amount of dCAT1 at the bilayer surface), and should be regarded as minimum possible values. Yet, there is a clear tendency of migration of the cationic spin label to the DMPG bilayer surface above T_m, as compared to the roughly constant value obtained for SDS at all temperatures. The electrostatic character of the force that drives dCAT1 to the DMPG vesicle surface was evinced by the decrease of dCAT1 membrane partitioning

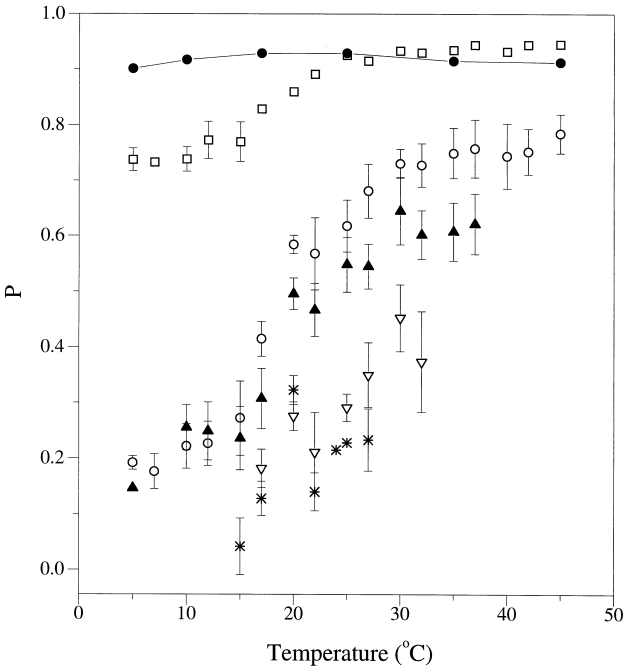

Fig. 3. Partition ratios (surface label moles/total label moles) calculated from the second integral ratio between the surface and the composite spectra. (●) 12.1 mM SDS in water; 10 mM DMPG in (□) pure water, (○) buffer (10 mM Hepes, pH 7.4); buffer plus (▲) 2 mM, (▽) 5 mM, and (*) 10 mM NaCl.

with the increase in ionic strength (Fig. 3). Accordingly, in DMPG–buffer dispersion with 100 mM NaCl, where the PG^- groups are partly shielded by the cations in solution, or in the neutral DMPG in low pH medium (pH 1), the dCAT1 spectra were identical to the free spectrum at all temperatures, that is, no surface label could be detected (data not shown).

For each ionic strength, partition ratios could be calculated up to a certain temperature, after which no simple decomposition could be obtained. This upper limit is the point at which data cease in Fig. 3: around 37°C, 32°C and 27°C, for the 2, 5 and 10 mM NaCl samples, respectively. Fig. 5 shows some attempts to decompose spectra at 35°C and 40°C. At 35°C the surface spectra of DMPG–water, DMPG–buffer, and DMPG–buffer+2 mM NaCl could be attributed to a single ESR signal, whereas for higher ionic strengths they could not. The resulting ESR spectra are more complex, indicating the presence of at least two different components. At 40°C, not even the spectrum in DMPG–buffer+

[1] 12.1 mM was a very convenient SDS concentration, as the spin label partitioned between the aqueous medium and the micellar surface. For SDS concentrations above 50 mM no free label could be detected. At 12.1 mM of SDS, on average, 8 mM is free and 4.1 mM is arranged in micelles [24]. It is important to note that dCAT1 in SDS samples below the CMC (around 8 mM) yielded ESR spectra identical to those obtained in pure aqueous solution (results not shown), showing that there is no label binding to SDS monomers or pre-micellar aggregates.

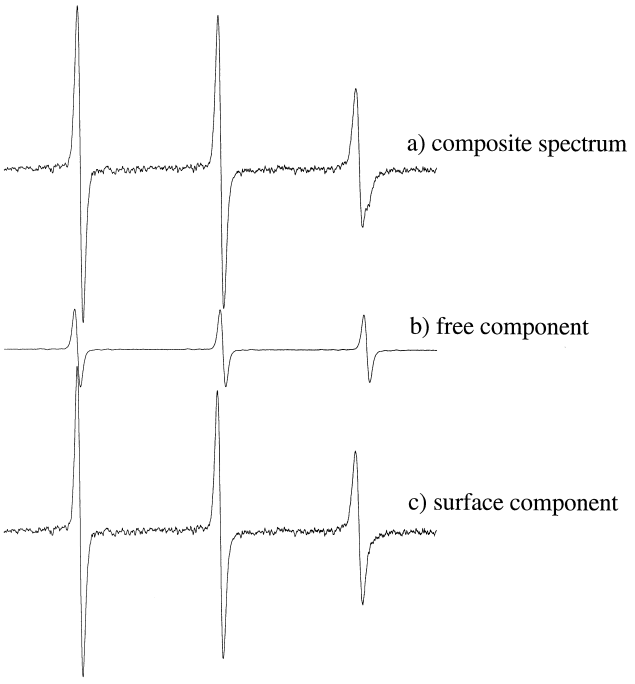

Fig. 4. SDS spectra subtraction: (a) 0.04 mM dCAT1 in 12.1 mM SDS in pure water; (b) dCAT1 free in buffer; (c) top minus middle. The free and surface components spectra are shown with the real relative intensities that they appear in the composite signal (a). Total spectra width 50 G, $T = 25$°C.

2 mM NaCl could be decomposed in one free and one surface component (Fig. 5). It is important to mention that, for each ionic strength, the number of surface spin labels (calculated from the second integral of the subtracted spectra) remained roughly unchanged for all temperatures above T_m, despite the complexity of the signal. Interestingly, the limiting temperatures for successful decomposition, were rather similar to the post-transition temperatures, for the different DMPG samples (see Fig. 1). These results might be a coincidence, or might be an indication of some kind of change at the DMPG vesicle surface at T_{post}, which is not yet understood.

Whenever a successful spectral decomposition was possible, the dCAT1 surface signal was least-squares fit to a Voigt line shape and the parameters analyzed according to [20,25], to yield isotropic hyperfine splitting values (a_o) and correlation times, parallel and perpendicular to the molecular symmetry axis ($\tau_{\|}$ and $\tau_{\perp}$). The same procedures were applied to spectra observed in SDS micelles. Fig. 6a,b compare the hyperfine splittings and correlation times for the free component as well as the surface component in different DMPG and SDS samples. The calculated $\tau_{\|}$ values for all samples are not shown in Fig. 6b because they were found to be small, similar to the $\tau_{\perp}$ values obtained for free dCAT1, at all temperatures.

It is interesting to use the well-known dependence of the hyperfine interaction parameter of nitroxyl radicals on polarity, to compare the a_o values and correlation times for dCAT1 in the several DMPG systems and SDS micelles. For the lipid samples, below T_m, the spin label is localized in a region with a dielectric constant very similar to that of bulk water (Fig. 6a), although its movement is somewhat more restricted, as indicated by the slightly higher $\tau_{\perp}$ values for the DMPG samples (Fig. 6b). Upon the main lipid transition, there is a significant increase in the dCAT1 $\tau_{\perp}$ values for all DMPG sam-

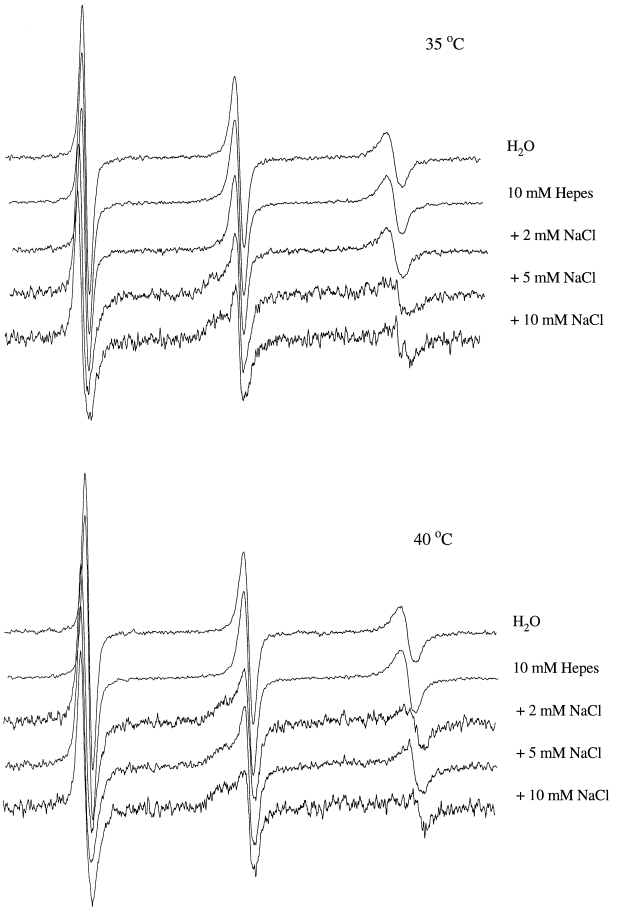

Fig. 5. ESR spectra of the surface component of 0.1 mM dCAT1 in the presence of 10 mM DMPG in different media at 35°C (top), and 40°C (bottom). Total spectra width 50 G.

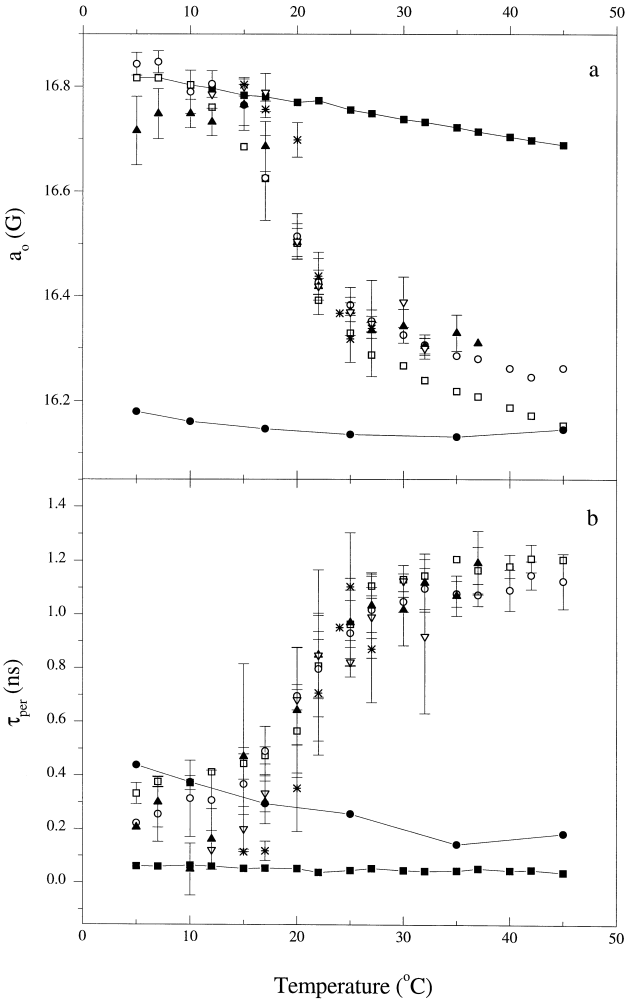

Fig. 6. Temperature dependence of the (a) isotropic hyperfine splitting values a_o, and (b) the perpendicular correlation time $\tau_\perp$, calculated from the ESR spectra of 0.1 mM dCAT1 (■), free in buffer (10 mM Hepes, pH 7.4), or from the surface component of dCAT1 in the presence of 10 mM DMPG in (□) pure water, (○) buffer, buffer plus (▲) 2 mM, (∇) 5 mM, and (*) 10 mM NaCl, and (●) 0.04 mM dCAT1 in 12.1 mM SDS in pure water.

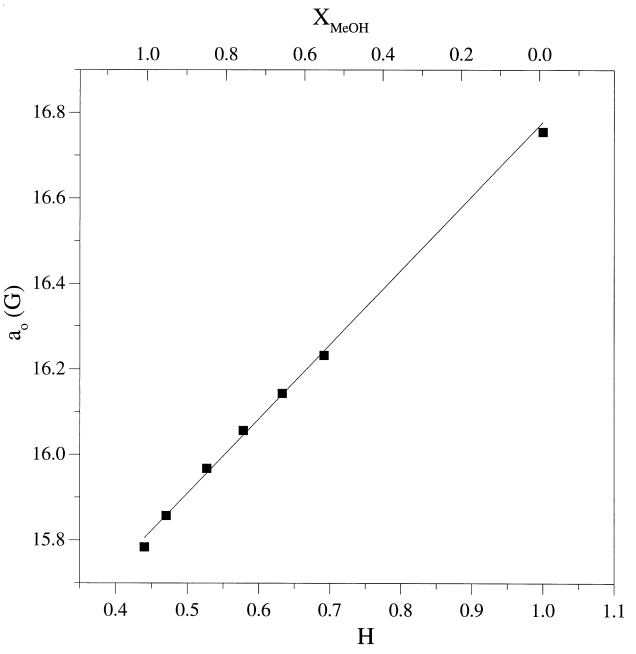

Fig. 7. The isotropic hyperfine splitting values (a_o) of dCAT1 as a function of the medium polarity index H (see text) calculated for different mixtures of methanol/water (X_{MeOH}), $T = 25$°C.

ples, indicating that the label penetrates somewhat further down the vesicle surface. Such a relocation could be due to a less packed membrane surface above T_m and would be in accord with the decreasing values of a_o above T_m since the deeper penetration of the label would locate it in a region of diminished polarity. In SDS micelles, the a_o values (Fig. 6a) show only a minor decrease with temperature so the dielectric constant of the microenvironment where dCAT1 is localized does not change much with temperature. The surface dCAT1 in SDS micelles is generally in a less polar microenvironment than the surface label in DMPG vesicle; the only exception being DMPG–water at high temperature. The perpendicular correlation times (Fig. 6b), in all DMPG systems, are much larger than they are in SDS, indicating a significant higher degree of spin label immobilization at the DMPG vesicle surface as compared to SDS micelles.

The dielectric constant of the site where the spin label is localized can be estimated by comparing the obtained a_o values with those yielded by the label in different mixtures of methanol/water. Fig. 7 shows the isotropic hyperfine constants calculated by the fitting of the dCAT1 ESR signals in different media, recorded at 25°C, as a function of the polarity index H [26]. The latter is defined as the ratio of the volume concentration of OH groups to that in water (55.4 mol/l) and calculated for the different mixtures of methanol/water used.[2] The polarity index H shows

[2] The values of H were calculated from a linear least-squares fit of the data given in Table 1 of [26]: $H(25°C) = 0.987 - 0.542X_{MeOH}$, where X_{MeOH} is the weight fraction of methanol.

an excellent linear correlation to other measures of polarity, for example, the dielectric constant [26]. The corresponding dielectric constants for the sites monitored by the surface dCAT1, at 25°C in DMPG ($a_o = 16.37$ G, $H = 0.77$) and in SDS ($a_o = 16.13$ G, $H = 0.63$), can be estimated [26] to be around 60 and 49, respectively.

4. Discussion

Considering that dCAT1 is a cationic highly aqueous soluble molecule, it probably does not penetrate vesicles and micelles, but resides on their surface, therefore causing minimum disturbance of the original vesicle structure. The shallow position of the label is confirmed by the relative high dielectric constant measured for its surface microenvironment [27]. For most samples the dCAT1 ESR signal could be ascribed to the label either free in solution or close to the negative surface of DMPG membrane. The appearance of two separate signals shows that the frequency of exchange between the two sites is low compared with the difference in resonance fields. This ability to report simultaneously on the surface of the vesicle and the bulk solution, its enhanced resolution due to the replacement of protons by deuterons, and its motionally narrowed spectra allowing precise determination of a_o and $\tau_\perp$, makes dCAT1 a very convenient probe for the surface electrostatic potential of an anionic amphiphilic vesicle.

Based on light scattering and conductivity measurements, it was previously proposed [12] that, at T_m, the melting of the hydrocarbon chains would trigger a process leading to an increase in the degree of DMPG vesicle surface ionization, with a corresponding increase in the magnitude of the negative surface potential. Particles with higher surface potentials would repel each other more strongly, allowing the electrostatic double layer repulsion to overcome the attractive van der Waals forces thereby favoring a non-aggregated dispersion. That would give rise to the observed increase in the sample conductivity and decrease in the intensity of light scattering at T_m (Fig. 1). In the present work, the migration of the cationic spin label to the DMPG bilayer surface above T_m (Fig. 3) would be in accord with the increase of the magnitude of the surface potential at T_m.

4.1. Two-sites partition model

To estimate the DMPG vesicle surface potential (Ψ_o) a simple calculation can be carried out, based on the experimental partition ratio, as shown in Section 2 (Eq. 1). The model assumes that the interaction between dCAT1 and DMPG vesicle surface is chiefly electrostatic. This reasoning is based on the absence of detectable dCAT1 close to the membrane either at high ionic strength or at low pH value, as mentioned before. It parallels the discussion made by [14] with an amphiphilic spin label, where the hydrophobic contribution was evaluated with a non charged membrane.

Table 1 shows the measured dCAT1 partition ratios in different systems, in the lipid liquid–crystal phase: 10 mM DMPG in water, 10 mM DMPG in 10 mM Hepes buffer (pH 7.4), at several ionic strengths, and 12.1 mM SDS in water. (No surface potential calculations were attempted for DMPG below T_m due to the relative inaccuracy of the spectral subtractions.) ψ_o was calculated assuming an area per lipid headgroup $A = 60$ Å^2 [28], $T = 303$ K, and the total number of lipids N calculated for a certain V_{total} of 10 mM DMPG. The same area per lipid headgroup was used for DMPG in water. Considering the dimensions of the dCAT1 molecule (roughly 6 Å along the N–O axis), 6 Å was used as an average value for the vesicle shell thickness h, though this point will be further discussed in the next section.

For SDS, 4.1 mM was calculated [24] to form

Table 1
DMPG vesicle surface potential (Ψ_o) calculated from Eq. 1, using the partition ratio (P = surface label moles/total label moles) of dCAT1 in lipid suspensions at different ionic strengths (n)

System	n (mM)	P	Ψ_o (mV)
DMPG in			
water	0.1	0.95	−237
buffer	4.0	0.75	−189
+2 mM NaCl	6.0	0.60	−171
+5 mM NaCl	9.0	0.40	−150
+10 mM NaCl	14.0	0.25	−132
SDS		0.90	−220

micelles, with an aggregation number of 50.6 and a diameter of 44 Å^2, yielding an area per lipid headgroup of 120 Å^2. The shell thickness was also assumed to be 6 Å [29].

It is interesting to point out that the ψ_o value obtained for SDS micelle is similar to those obtained for DMPG in low ionic strength, and rather higher than the values obtained for SDS micelles with fluorescent probes, around −150 mV [30]. One has to take into account that the fluorescent probes used were anchored into the SDS micelle, due to their hydrophobic chain, perhaps probing a different region of the micelle as compared to dCAT1, although the estimated dielectric constant by fluorescence, $\varepsilon \approx 50$ [30], was similar to the one calculated with dCAT1 ($\varepsilon = 49$). On the other hand, the fluorescent probes could be perturbing the original SDS aggregate as they partition inside it, unlike dCAT1 which is likely to reside on the micelle's surface. It has also to be considered that micelles have a rather rough surface, where a single surface potential might not apply.

As expected, there is a decrease in the magnitude of the DMPG surface potential with the increase of the ionic strength. It is important to note that the methodology used here is restricted to partition ratios in the experimentally measurable interval of 0.10 to 0.95. For 10 mM DMPG, in the liquid–crystalline phase, it corresponds to 103 mV $< |\psi_o| <$ 237 mV. That limitation is clearly seen in the case of DMPG with 100 mM NaCl, where $P \approx 0$, which could correspond to a surface potential around −100 mV, as suggested before [12,31].

Although we have assumed that the variation in the partition ratio, P, at T_m is caused by a change in the surface potential only, it can be seen in Eq. 1 that an increase in the area available for label binding would also induce an increase in the partition ratio P, even for constant surface potential. However, a rough estimation of a possible variation in the available area at T_m tends to exclude that last hypothesis, as follows. The expected increase in area upon the main phase transition (48 to 60 Å^2) would not increase the partition ratio more than 10%. On the other hand, if we consider the molecular masses calculated by the Zimm plot for the DMPG aggregates, below and above T_m, 60 and 15 MDa, respectively [12], we may estimate that an aggregate of around four vesicles fall apart at T_m. Considering the close packing of four spheres, and considering that each one has around 60° of solid angle not available for external binding, not more than 1/15 of each vesicle area would be inaccessible to the label. This estimate is an upper limit since it supposes that the rather small dCAT1 could not access any area inside the contact points. Even this upper limit in the change in area would not affect P more than about 7%. Perhaps other structures for the DMPG vesicles decrease the accessible area upon aggregation to an extend that could not be completely neglected.

4.2. Gouy–Chapman–Stern model

The Ψ_o values obtained for DMPG can be compared to those calculated by the Gouy–Chapman–Stern model (Eq. 3), here called Ψ_o^{GCS}, where the area per lipid headgroup was the same one used before, namely $A = 60$ Å^2, and ε was assumed to be 80, as the model assumes the same dielectric constant up to the membrane surface. Fig. 8 shows the dependence of Ψ_o with the sample ionic strength, and compares its variation with two theoretical curves

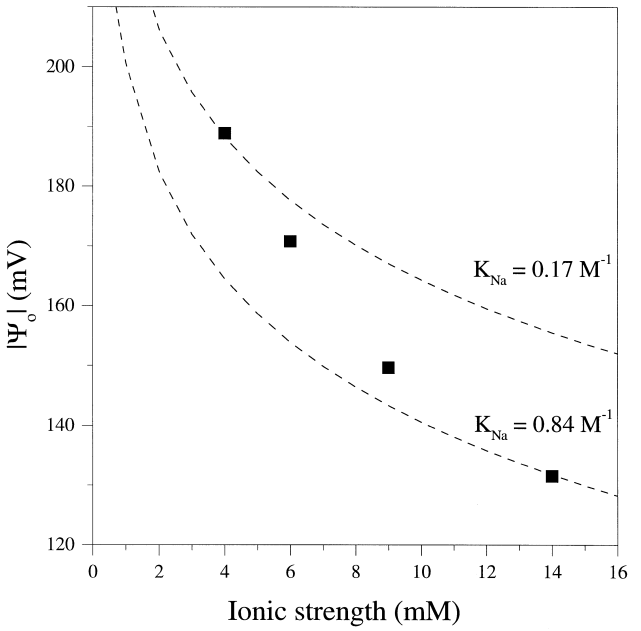

Fig. 8. Ionic strength dependence of the electrostatic surface potential: (■) experimental values calculated from the partition ratios; (dashed lines) theoretical values predicted by the Gouy–Chapman–Stern model for two different PG^-–Na^+ binding constants.

($|\Psi_o^{GCS}|$ from Eq. 3, dashed lines) calculated for two different K_{Na} values, 0.17 M^{-1} and 0.84 M^{-1}, which correspond to α values 0.52 and 0.33, respectively.[3] It is evident that there is no constant value of K_{Na} which yields good agreement with the surface potential values calculated from the experimental data, Ψ_o, assuming a fixed value for the shell thickness h. Whereas the magnitudes of the potentials yielded by the two methodologies are not very different, the experimental decrease of the surface potential with ionic strength, for any given value of h, is steeper than that predicted by the model. This could possibly be attributed to the various approximations in the Gouy–Chapman–Stern model, like the uniform charge distribution over a planar surface, the point character of the charged particles, and the sharp discontinuity of the dielectric constant[4] at the vesicle surface, although some of them were found rather good for highly charged surfaces [33]. It is important to note that the different behavior of the two methodologies could possibly be relevant only in the low ionic strength range used here, where the interaction between charged monolayers, either from the same vesicle or from neighboring ones, cannot be completely dismissed.

On the other hand, one could consider the possibility of the variation of the average thickness h with the ionic strength, therefore introducing a correction in the values of ψ_o calculated from the measured partition ratios. Interestingly, if it is assumed that h decreases with ionic strength proportionally to the variation of the Debye length,[5] a relatively good correlation can be obtained between the two methods discussed here, namely, the two sites and the Gouy–Chapman–Stern models. For instance, the Ψ_o^{GCS} profile obtained for $K_{Na} = 0.84$ M^{-1} could be reasonably well reproduced by varying the h value from 9.4 Å ($n = 4$ mM) to 5 Å ($n = 14$ mM). However, the rather similar values obtained for the ESR parameters of the dCAT1 surface component in the different ionic strength samples (Fig. 6; a_o and τ, indicating the label microenvironment dielectric constant and mobility, respectively) do not suggest a dependence of the spin label average position with the medium ionic strength. The above discussion comparing the two methodologies does certainly need further consideration.

The Gouy–Chapman–Stern model presented here includes the binding of sodium ions to the phosphate groups of DMPG membranes. The K_{Na} values, 0.17 M^{-1} and 0.84 M^{-1}, though very different, are in the range of the sodium binding constants proposed in the literature (see [12] and references therein). Although many authors do not consider the binding of Na^+ to DMPG vesicle surface, and keep $\alpha = 1$, the consideration of $K_{Na} \neq 0$ may be rather relevant.[6] As suggested before [12], the lower value of K_{Na} for DMPG in the liquid–crystal phase, as compared to the gel phase, would explain the higher surface potential and higher repulsion among the lipid vesicles, and, consequently, the lower intensity of light scattering for temperatures above T_m. It is interesting to mention the work by Eklund et al. [34] where it was found that sodium ions induced aggregation in DMPG vesicles (at low lipid concentration, 0.14 mM, and high salt concentration, 600 mM) only for samples at low temperature, below T_m. Hence, their results also seem to indicate a higher Na^+ binding constant for the lipid in the gel phase as compared to the liquid–crystal phase.

In the above discussions the binding of dCAT1 to DMPG molecules was neglected. Apart from the arguments given in the last section, concerning the ab-

[3] K_H was assumed to be 15.8 M^{-1} according to [32], or calculated from [2]. Although α is a function of the ionic strength (Eq. 4), for the pH and n values used here $[H^+]_\infty \ll n$, and $[Na^+]_\infty \approx n$, therefore α is effectively independent of n.

[4] it is interesting to note that, though some theoretical models assume the sharp discontinuity of ε at the bilayer surface, and/or that ions do not penetrate the membrane polar region, it is shown here that the bulky ion dCAT1 (or at least its NO group) resides in a region of $\varepsilon \approx 60$.

[5] The Debye screening length, given by

$$\frac{1}{\kappa} = \left(\frac{\varepsilon\varepsilon_o kT}{2e^2 N_A n}\right)^{1/2}$$

(see parameter definitions in Section 2) gives an estimation of the length of the diffuse double layer at the vesicle surface [23].

[6] For instance, the necessity to overestimate the area per lipid molecule (120 $Å^2$ as compared to 48 $Å^2$ determined by X-ray diffraction) in the fitting of the experimentally measured electrostatic potential of DMPG in the gel phase [16], could be overcome by the use of $\alpha = 0.4$, which would correspond to $K_{Na} = 0.46$ M^{-1}.

sence of a detectable population of a less mobile dCAT1 in the presence of low surface potential DMPG vesicles, it is important to consider the following reasoning. The binding constant PG^-–$dCAT1^+$, K_{dCAT1}, was found to be lower than K_{Na}, as 2 mM dCAT1 does not cause any change in the DMPG post-transition temperature, T_{post}, measured by light scattering (result not shown), compared to the large shift observed in the presence of 2 mM NaCl (see Fig. 1). Moreover, even if it is assumed that K_{dCAT1} is close to the K_{Na} value, i.e., around 0.8 M^{-1}, due to the low spin label concentration (0.1 mM) the surface potential value in the presence of dCAT1 will change less than 1%, and the amount of 'bound' dCAT1 would be negligible compared to the concentration at the surface and in solution.

4.3. DMPG in water

In the absence of added salt, multi-angle light scattering experiment indicated a strong interparticle correlation for DMPG in pure water [12]. That would be in accord with the Gouy–Chapman–Stern model ($n = 0.0025$ mM, due to protons only), which yields an $\alpha = 0.14$, and $\Psi_o^{GCS} = -317$ mV. However, in the present work, the 0.1 mM concentration of the charged dCAT1 has to be considered (for the DMPG–Hepes samples the concentration of dCAT1 was negligible compared to the other ions in solution). By solving Eq. 4 (in Section 2), considering $[Na^+]_\infty = 0$, $K_{dCAT1} = 0$, and $n = 0.1$ mM, an α value of 0.39 was found, which corresponds to $\Psi_o^{GCS} = -276$ mV, to be compared with -240 mV, obtained from the partition ratio. That difference could possibly be due to the sharp dependence of Ψ_o^{GCS} with the ionic strength, for very low n values, and, in the present case, the coarse Gouy–Chapman approximations of considering dCAT1 as a point charge, and non-interacting charged layers.

It is interesting to point out that DMPG in pure water has been shown to present some properties different from the lipid in buffered medium [8,12]. For instance, in water DMPG does not show a sharp lipid thermal transition, though spin labels intercalated in the hydrocarbon chains monitor regions of similar microviscosities, both at low (15°C, the gel phase) and high temperatures (40°C, the liquid–crystal phase), for all DMPG samples. As for the aggregate surface monitored here, the a_o values of dCAT1 in DMPG in buffer and in SDS micelles remain rather constant for higher temperatures, whereas there is a clear decrease of the a_o value, and consequently of the dielectric constant of the region where dCAT1 resides in DMPG in pure water (Fig. 6a). That could indicate structural changes in the vesicle provoked by increasing the temperature, allowing a slightly deeper penetration of the label. On the other hand, that possible variation on the vesicle structure is not reflected in the measurements of the label microenvironment viscosity, as the surface dCAT1 $\tau_\parallel$ and $\tau_\perp$ values remain rather constant above T_m, and very similar for all the DMPG samples, either in water or in buffer (Fig. 6b).

4.4. No evidence of membrane fusion

To test whether there was vesicle fusion at either T_m or T_{post}, the following experiment was carried out. A phospholipid spin label (16-PCSL), which shows negligible partition into the aqueous medium, incorporated in 10 mM DMPG dispersion was used in a concentration high enough to yield a spectrum broadened by spin exchange (3% of the lipid concentration, in moles). One volume of that dispersion was mixed with two volumes of a DMPG sample in the same concentration, but without the spin label. Therefore, if fusion occurred, a significant linewidth decrease would be expected, corresponding to the dilution of the spin label. No decrease in the spin exchange was observed during and after the following temperature cycle: 1 h at 25°C, 1 h at 40°C, 1 h at 17°C and back to 25°C. That experiment indicated that the spin labeled phospholipid could not spread out through the DMPG vesicles added afterwards, which would be expected if fusion had occurred.

5. Conclusions

The present work indicates that there is an increase in the DMPG vesicle surface potential at the lipid gel–liquid crystal transition, with accompanying penetration of the aqueous soluble cationic spin label dCAT1 into the surface shell, to a region of dielectric constant about 60. Although there were modifications in the ESR spectra of dCAT1 close to the

DMPG bilayer at T_{post}, no simple conclusion could be drawn due to the complexity of the signal. The surface component spectra obtained for temperatures above T_{post} (Fig. 5) could be possibly attributed to more than one site at the vesicle surface, or different vesicle structures present in the dispersion.

The spin label dCAT1 seems a rather promising probe in the general study of surface electrical potential of anionic amphiphilic aggregates. Its aqueous soluble character together with its positive charge, are likely to allow the probing of the surface without altering much the original structure of the aggregates. The decomposition of the dCAT1 ESR spectra into two signals, one more restricted (at the surface) and one free, allows not only the estimation of the surface potential, based on the two sites model used here, but also an analysis of the surface signal, providing information about the surface packing and local dielectric constant. That methodology could be extended to the study of the binding of small molecules, like biological relevant peptides, to lipid bilayers. It would be interesting to see how they alter the membrane surface potential and packing, and, based on these alterations, to discuss partition coefficients of charged drugs to anionic or neutral surfaces.

Acknowledgements

This work was supported by USP, FAPESP, CNPq and FINEP. B.L.B, M.T.L.F. and O.R.N thank USP and FAPESP for traveling support. B.L.B. was supported by the grant NIH S06 GM/HD48680-03. We are grateful to Dr. V.B. Henriques and to Dr. C. Goldman for very helpful discussions.

References

[1] R.B. Gennis, Biomembranes. Molecular Structure and Function, Springer, New York, 1989.
[2] A. Watts, K. Harlos, W. Maschke, D. Marsh, Control of the structure and fluidity of phosphatidylglycerol bilayers by pH titration, Biochim. Biophys. Acta 510 (1978) 63–74.
[3] J. Seelig, P.M. MacDonald, P.G. Scherer, Phospholipid head groups as sensors of electric charge in membranes, Biochemistry 26 (1987) 7535–7541.
[4] T. Heimburg, R.L. Biltonen, Thermotropic behavior of dimyristoylphosphatidylglycerol and its interaction with cytochrome c, Biochemistry 33 (1994) 9477–9488.
[5] M.H. Biaggi, K.A. Riske, M.T. Lamy-Freund, Melanotropic peptides–lipid bilayer interaction. Comparison of the hormone α-MSH to a biologically more potent analog, Biophys. Chem. 67 (1997) 139–149.
[6] A. Watts, D. Marsh, Saturation transfer ESR studies of molecular motion in phosphatidylglycerol bilayers in the gel phase: effects of pretransition and pH titration, Biochim. Biophys. Acta 642 (1981) 321–341.
[7] R.M. Epand, B. Gabel, R.F. Epand, A. Sen, S.W. Hui, Formation of a new stable phase of phosphatidylglycerol, Biophys. J. 63 (1992) 327–332.
[8] R.M. Epand, S.W. Hui, Effect of electrostatic repulsion on the morphology and thermotropic transitions of anionic phospholipids, FEBS Lett. 209 (1986) 257–260.
[9] N.L. Gershfeld, W.F. Stevens Jr., R.J. Nossal, Equilibrium studies of phospholipids bilayer assembly, Faraday Discuss. Chem. Soc. 81 (1986) 19–28.
[10] I.S. Salonen, K.K. Eklund, J.A. Virtanen, P.K.J. Kinnunen, Comparison of the effects of NaCl on the thermotropic behaviour of *sn*-1′ and *sn*-3′ stereoisomers of 1,2-dimyristoyl-*sn*-glycero-3-phosphatidylglycerol, Biochim. Biophys. Acta 982 (1989) 205–215.
[11] M. Kodama, T. Miyata, T. Yokoyama, Crystalline cylindrical structures of Na^+-bound dimyristoylphosphatidylglycerol as revealed by microcalorimetry and electron microscopy, Biochim. Biophys. Acta 1168 (1993) 243–248.
[12] K.A. Riske, M.J. Politi, W.F. Reed, M.T. Lamy-Freund, Temperature and ionic strength dependent light scattering of DMPG dispersions, Chem. Phys. Lipids 89 (1997) 31–44.
[13] Y.P. Zhang, R.N.A.H. Lewis, R.N. McElhaney, Calorimetric and spectroscopic studies of the thermotropic phase behaviour of the n-saturated 1,2-diacylphosphatidylglycerols, Biophys. J. 72 (1997) 779–793.
[14] J.D. Castle, W.L. Hubbell, Estimation of membrane surface potential and charge density from the phase equilibrium of a paramagnetic amphiphile, Biochemistry 15 (1976) 4818–4831.
[15] S.C. Hartsel, D.S. Cafiso, Test of discreteness-of-charge effects in phospholipid vesicles: measurements using paramagnetic amphiphiles, Biochemistry 25 (1986) 8214–8219.
[16] V.V. Khramstov, D. Marsh, L. Weiner, V.A. Reznikov, The application of pH-sensitive spin labels to studies of surface potential and polarity of phospholipid membranes and proteins, Biochim. Biophys. Acta 1104 (1992) 317–324.
[17] J.C. Franklin, D.S. Cafiso, R.F. Flewelling, W.L. Hubbell, Probes of membrane electrostatics: synthesis and voltage-dependent partitioning of negative hydrophobic ion spin labels in lipid vesicles, Biophys. J. 64 (1993) 642–653.
[18] R.F. Epand, R. Kraayenhof, G.J. Sterk, H.W.W.F. Sang, R.M. Epand, Fluorescent probes of membrane surface properties, Biochim. Biophys. Acta 1284 (1996) 191–195.
[19] E.K. Krasnowska, E. Gratton, T. Parasassi, Prodan as a

membrane surface fluorescence probe: partitioning between water and phospholipid phases, Biophys. J. 74 (1998) 1984–1993.
[20] B.L. Bales, Inhomogeneously broadened spin-label spectra, in: L.J. Berliner, J. Reuben (Eds.), Biological Magnetic Resonance, vol. 8, Plenum, New York, 1989, pp. 77–129.
[21] B.L. Bales, M. Peric, M.T. Lamy-Freund, Contributions to the gaussian line broadening of the proxyl spin probe EPR spectrum due to magnetic-field modulation and unresolved proton hyperfine structure, J. Magn. Reson. 132 (1998) 279–286.
[22] H.J. Halpern, M. Peric, C. Yu, B. Bales, Rapid quantitation of parameters from inhomogeneously broadened EPR spectra, J. Magn. Reson. 103 (1993) 13–22.
[23] D.F. Evans, H. Wennerstöm, Electrostatic interactions in colloidal systems, in: The Colloidal Domain, Where Physics, Chemistry, Biology, and Technology Meet, VCH, New York, 1994, pp. 110–114.
[24] F.H. Quina, P.M. Nassar, J.B.S. Bonilha, B.L. Bales, Growth of sodium dodecyl sulfate micelles with detergent concentration, J. Phys. Chem. 99 (1995) 17028–17031.
[25] D. Marsh, Experimental methods in spin-label spectral analysis, in: L.J. Berliner, J. Reuben (Eds.), Biological Magnetic Resonance, vol. 8, Plenum, New York, 1989, pp. 255–303.
[26] P. Mukerjee, C. Ramachandran, R.A. Pyter, Solvent effects on the visible spectra of nitroxides and relation to nitrogen hyperfine splitting constants. Nonempirical polarity scales for aprotic and hydroxylic solvents, J. Phys. Chem. 86 (1982) 3189–3197.
[27] S. Mazères, V. Schram, J.-F. Tocanne, A. Lopez, 7-Nitrobenz-2-oxa-1,3-diazole-4-yl-labeled phospholipids in lipid membranes: differences in fluorescence behavior, Biophys. J. 71 (1996) 327–335.
[28] D. Marsh, An interaction spin label study of lateral expansion in dipalmitoyllecithin-cholesterol bilayers, Biochim. Biophys. Acta 363 (1974) 373–386.
[29] B. Cabane, R. Duplessix, T. Zemb, High resolution neutron scattering on ionic surfactant micelles: SDS in water, J. Physique 46 (1985) 2161–2178.
[30] F. Griser, C.J. Drummond, The physicochemical properties of self-assembled surfactant aggregates as determined by some molecular spectroscopic probe technique, J. Phys. Chem. 92 (1988) 5580–5593.
[31] G. Cevc, A. Watts, D. Marsh, Non-electrostatic contribution to the titration of the ordered-fluid phase transition of phosphatidylglycerol bilayers, FEBS Lett. 120 (1980) 267–270.
[32] K. Toko, K. Yamafuji, Influence of monovalent and divalent cations on the surface area of phosphatidylglycerol monolayers, Chem. Phys. Lipids 26 (1980) 79–99.
[33] R.M. Peitzsch, M. Eisenberg, K.A. Sharp, S. McLaughlin, Calculations of the electrostatic potential adjacent to model phospholipid bilayers, Biophys. J. 68 (1995) 729–738.
[34] K.K. Eklund, J.A. Virtanen, K. Vuori, J. Patrikainen, P.K.J. Kinnunen, Role of the polar head group stereoconfiguration in the cation-induced aggregation of dimyristoylphosphatidylglycerol vesicles, Biochemistry 26 (1987) 7542–7545.